interferon-induced protein 44-like (IFI44L), 2′-5′-oligoadenylate synthetase 2 (OAS2), ubiquitin specific peptidase 18 (USP18), radical S-adenosyl methionine domain containing 2 (RSAD2), interferon-induced protein with tetratricopeptide repeats 1 (IFIT1), interferon induced with helicase C domain 1 (IFIH1), XIAP associated factor 1 (XAF1), cytidine monophosphate (UMP-CMP) kinase 2, mitochondrial (CMPK2), epithelial stromal interaction 1 (EPSTI1), hect domain and RLD 6 (HERC6), poly (ADP-ribose) polymerase family, member 9 (PARP9), phospholipid scramblase 1 (PLSCR1), and glyceraldehyde-3-phosphate dehydrogenase (GAPDH) were obtained from the TaqMan assay reagents library. Primer pairs and probes for IL28B were designed as previously described.[12] The standard curve was obtained in every assay using the RNA obtained from a normal liver.[14,15] The expression values were normalized by GAPDH, and normalized values indicate the relative fold expression to a normal liver.

Amino Acid Substitutions of ISDR in the Nonstructural 5A Region

The nucleotide sequence of ISDR in the nonstructural 5A region was determined by direct sequencing of PCR amplified materials.[4] Mutant-type ISDR was defined as containing 2 or more aa substitutions.

Genetic Variation of IL28B Polymorphism

A single nucleotide polymorphism (SNP) of IL28B was evaluated in 91 patients whose hepatic gene expression profiling was obtained. We genotyped 32 patients using Affymetrix Genome-Wide Human SNP Array 6.0 as previously described.[12] The results for rs8105790, rs11881222, rs8099917, and rs7248668 were retrieved from a database to evaluate the association of these SNPs. rs12979860 was determined by direct sequencing, and rs8099917 was determined using TaqMan Pre-Designed SNP Genotyping Assays (PE Applied Biosystems) as recommended by the manufacturer.

Statistical Analysis

The Mann-Whitney U test was used to analyze continuous variables. Fisher exact test and χ^2 test were used for the analysis of categorical data. The overall plausibility of the treatment response groups was assessed using Fisher C statistic (Supplementary Table 2).[16,17] C is defined by $C = -2 \sum \ln(p_i)$, where p_i is the probability (P value) of each independent statement (clinical factors). C follows a χ^2 distribution with 2k degrees of freedom, k being the number of independent statements (clinical factors).[16] A nonsignificant C value means that the treatment response in the 2 groups was not statistically independent.

Multivariate analysis was performed using a stepwise logistic regression model. Each cut-off point for the continuous variables was decided by analysis of the receiver operating characteristic (ROC) curve. A P value of less than .05 was considered significant. Statistical analyses were performed using JMP7 for Windows (SAS Institute, Cary, NC).

Results

Response Rate and Clinical Characteristics

The clinical characteristics of the patients are shown in Table 1 and Supplementary Table 1. All of the patients were infected with HCV genotype 1b and had a high viral load (>100K IU/mL). No patients were coinfected with the hepatitis B virus (HBV). The intention-to-treat analysis showed that SVR, TR, and NR were observed in 70 (42%), 55 (33%), and 43 (25%) patients, respectively (Supplementary Table 1). Before comparing patients with 3 different responses, the overall plausibility of the treatment response groups was assessed using Fisher C statistic. Fisher C statistic utilizes the P values obtained by comparing pretreatment factors including age, gender, liver factors, laboratory parameters, and viral factors. Because the SVR and TR groups could not be defined as different, they were grouped together and compared with NR (Table 1, Supplementary Table 2).

Eleven patients with NR discontinued the therapy after 24 weeks because of an insufficient effect, namely, serum HCV-RNA was still detectable at this time. The remaining patients completed 48 weeks of Peg-IFN and RBV combination therapy. The administration rate of Peg-IFN with 80% or more was achieved in 67% of patients, and the administration rate of RBV with 80% or more was achieved in 60% of patients (Table 1).

Analysis of Hepatic Gene Expression

Prior to treatment, 91 of 168 patients (Supplementary Table 3) were randomly selected, and their hepatic gene expression was determined using Affymetrix genechip analysis.

Hierarchical clustering using 37 representative ISGs (see Materials and Methods) demonstrated 2 clear clusters of patients: one was a group composed of patients with up-regulated ISGs (Up-ISGs), and the other was a group consisting of patients with down-regulated ISGs (Down-ISGs) (Figure 1). In patients with Up-ISGs, 21 (49%) showed NR, whereas 8 (17%) patients with Down-ISGs showed NR ($P = .002$). In contrast, 14 (33%) patients with Up-ISGs showed SVR, whereas 27 (56%) patients with Down-ISGs showed SVR ($P = .03$). There were no significant differences in the frequency of advanced stages of liver fibrosis (F3-F4) between patients with Up-ISGs and patients with Down-ISGs (18 [42%] and 17 [35%], respectively, $P = .664$). These data indicated that the up-regulation of ISGs in the liver before treatment was strongly associated with resistance to IFN treatment.

Host and Viral Factors Associated With the Response to Combination Therapy

To evaluate the multiple host and viral factors associated with the response to Peg-IFN and RBV combination therapy in all patients, univariate and multivariate analyses were performed. To assess the expression of hepatic ISGs, 15 genes (Mx1, OAS3, IFI44, IFI44L, OAS2,

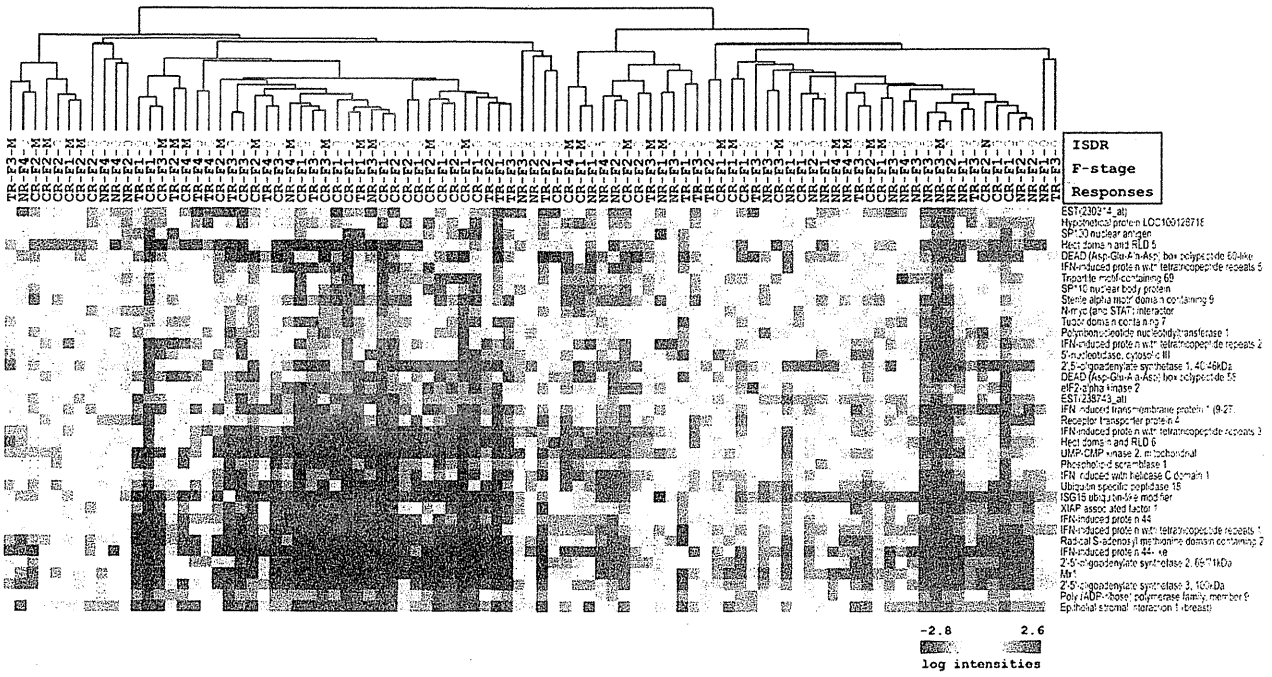

Figure 1. Hierarchical clustering analysis of 91 patients using 37 representative ISGs. Responses to therapy (SVR, TR, and NR), fibrosis stage (F1–F4), and status; ISDR mutations are also shown. ISDR mutation ≥2 = M, ≤1 = 0.

USP18, RSAD2, IFIT1, IFIH1, XAF1, CMPK2, EPSTI1, HERC6, PARP9, and PLSCR1) out of 37 representative ISGs were selected for their expression values of probe intensity, and their expression was confirmed in liver tissue obtained from 168 patients by RTD-PCR. Although there were significant correlations of their expression with each other, except RARP9 and PLSCR1 (Supplementary Table 4), the dynamic range of gene expression was high for 3 genes, namely, Mx1, IFI44, and IFIT1 (Supplementary Figure 1*A*). We averaged the expression values of Mx1, IFI44, and IFIT1 and used them for further study.

When we compared patients with SVR+TR and NR, the fibrosis stage of the liver ($P = .001$), expression of hepatic ISGs ($P < .001$), aspartate aminotransferase (AST) serum level ($P = .017$), γ-glutamyl transpeptidase (γ-GTP) ($P < .001$), low-density lipoprotein cholestrol (LDL-Chol) ($P = .019$), and insulin (μU/mL) ($P = .039$) were significantly different prior to treatment (Table 1). For treatment factors, the total dose and administration of IFN and RBV were not significantly different between these 2 groups. EVR was observed in 101 (81%) patients, and the proportion was significantly different ($P < .001$) between patients with SVR+TR and NR (Table 1).

Regression analysis of pretreatment factors showed a strong correlation among γ-GTP, alanine aminotransferase (ALT), and aspartate aminotransferase (AST); and homeostasis model assessment-insulin resistance (HOMA-IR), fasting blood sugar, and insulin; and total cholesterol (T-Chol), high-density lipoprotein cholestrol (HDL-Chol), and LDL-Chol (data not shown). We selected fibrosis stage, ISGs, HCV-RNA, ISDR mutation, and body mass index (BMI) as factors for multivariate analysis. Stepwise multivariate logistic regression analysis was performed using the selected factors. From the ROC curve, we set the cut-off value for the expression of ISGs as 3.5 (Supplementary Figure 1*B*). The results showed that expression of hepatic ISGs (<3.5), fibrosis stage (F1-F2), and ISDR mutation (≥2) were significant pretreatment factors contributing to SVR+TR (Table 1).

Clinical Parameters Associated With the Expression of Hepatic ISGs

Univariate and multivariate analyses revealed that the expression of hepatic ISGs was a strong predictor of the treatment outcome for SVR+TR patients. We next examined which clinical parameters were associated with the expression of hepatic ISGs (Table 2). Univariate analysis showed that the expression of ISGs was strongly correlated with the serum levels of γ-GTP ($P < .001$) and AST ($P < .001$) and weakly correlated with HCV-RNA, fasting blood sugar, insulin, HOMA-IR, triglyceride (TG), and LDL-Chol. Multivariate analysis showed that γ-GTP ($P < .001$), HCV-RNA ($P < .001$), and LDL-Chol ($P = .048$) were significantly associated with hepatic ISGs. Noticeably, the expression of ISGs was negatively correlated with HCV-RNA in SVR+TR patients ($P = .009$), whereas this correlation was not evident in NR patients ($P = .298$) (Table 2, Supplementary Figure 2). These results may indicate that endogenous ISGs suppress HCV in SVR+TR patients, whereas they are not active in NR patients.

Table 2. Clinical Factors Associated With Expression of Hepatic Interferon-Stimulated Genes

	Univariate analysis				Multivariate analysis			
Clinical factor	β	95% CI		*P* value	β	95% CI		*P* value
AST (*IU/L*)	0.274	0.13	0.42	<.001	—	—	—	
γ-GTP (*IU/L*)	0.326	0.18	0.47	<.001	0.288	0.14	0.43	<.001
HCV-RNA (*KIU/mL*)	−0.170	−3.19	−0.02	.025	−0.255	−0.40	−0.11	<.001
SVR+TR	−0.237	−0.32	−0.05	.009	—	—	—	
NR	−0.168	−0.57	0.18	.298	—	—	—	
FBS (*mg/dL*)	0.182	0.03	0.35	.021	—	—	—	
Insulin (*μU/mL*)	0.190	0.03	0.34	.016	—	—	—	
HOMA-IR	0.181	0.03	0.33	.017	—	—	—	.073
TG (*mg/dL*)	0.201	0.05	0.35	.011	—	—	—	.089
LDL-Chol (*mg/dL*)	−0.177	−0.33	−0.02	.025	−0.143	−0.28	0.00	.048

γ-GTP, γ-glutamyl transpeptidase; AST, aspartate aminotransferase; FBS, fasting blood sugar; TG, triglycerides; TR, transient response; NR, no response; SVR, sustained viral response; HOMA-IR, homeostasis model assessment of insulin resistance; LDL-chol, low-density lipoprotein cholesterol; CI, confidence interval; β, β coefficient; CI, confidence interval.

Expression of Hepatic ISGs Before Treatment Is Associated With Genetic Variation of IL28B

Recently, a GWAS successfully identified the genomic locus associated with the treatment response to Peg-IFN and RVB combination therapy for CH-C. Genetic variation in IL28B predicts HCV treatment-induced viral clearance.[11,12] We determined the genetic variation in IL28B of 32 patients[12] (Table 3). The SNPs rs8105790, rs11881222, rs8099917, and rs7248668 had a significant association with treatment response (odds ratio: 24.7–27.1, $P = 1.84 \times 10^{-30}$–2.68×10^{-32}). These SNPs are located in block 2 of the IL28B haplotype and show significant linkage disequilibrium in the HapMap data.[12] Ge et al[11] reported a different SNP (rs12979860) that was located between rs11881222 and rs8099917. The nucleotide sequence of rs12979860 was determined by direct sequencing, and the results are shown in Table 3. There was a strong association of rs12979860 and the other 4 SNPs indicating that this SNP was located within the same haplotype block. We confirmed these findings in multiple samples from Japanese patients (data not shown).

We selected rs8099917 for further study and evaluated it using TaqMan Pre-Designed SNP Genotyping Assays. The G nucleotide of rs8099917 was associated with a poor response to treatment (minor allele), whereas the T was associated with a fair response to treatment (major allele).[12] Out of 91 patients (Supplementary Table 3), the proportion of major homozygotes (TT), heterozygotes (TG), and minor homozygotes (GG) were 66% (60/91), 30% (27/91), and 4% (4/91), respectively (Table 4); 86% (51/60) of the major genotype (TT) patients had SVR or TR, whereas 65% (20/31) with the minor genotypes (TG or GG) had NR ($P < .001$).

Interestingly, hepatic gene expression profiles revealed that patients with the minor genotype showed higher expression of hepatic ISGs, whereas patients with the major genotype showed lower expression of hepatic ISGs (Figures 2 and 3). To examine further the relationship of the genetic variation in IL28B and its expression levels, we evaluated the expression of IL28B in the liver by RTD-PCR (Figure 3). IL28B expression was approximately 10-fold less than the expression of ISGs. Although IL28B expression tended to be higher in some patients with the major genotype, there was no significant difference in IL28B expression in the liver between the major and minor genotypes (Figure 3*A*). Nevertheless, the expression of ISGs was clearly high in patients with the minor genotype ($P < .0001$) (Figure 3*B*). IL28 activates signal tranducers and activators of transcription 1 (STAT1) through downstream signaling from a heterodimeric class II cytokine receptor that consists of IL-10 receptor β (IL-10Rβ) and IL-28 receptor α (IL-28Rα).[18,19] Therefore, we examined the correlation between the expression of IL28B and ISGs. IL28B expression correlated with the expression of ISGs ($r = 0.44$, $P < .001$); however, the correlation was different according to the SNP genotype. We observed a steep-slope correlation for the minor genotype and a slow-slope correlation for the major genotype (Figure 3*C* and *D*). Interestingly, 4 minor homozygotic (GG) patients showed a steeper correlation than the heterozygotes (TG) (Figure 3*D*). Thus, the IL28B polymorphism might differentially regulate the expression of ISGs in the liver, leading to the different treatment outcomes.

We performed univariate and multivariate analyses to identify the clinical factors associated with the major and minor genotypes (Table 4). Univariate analysis showed that higher hepatic ISGs and lower body mass index were significantly associated with the minor genotype; however, multivariate analysis showed that only hepatic ISGs (≥3.5) were associated with the minor genotype ($P < .001$; OR, 18.1; 95% confidence interval: 3.95–113). We further compared the predictive capacity of multivariate models using the expression of hepatic ISGs (<3.5 vs ≥3.5) or the IL28B genotype (major vs minor) (Supplementary Table 6). The predictive performance and fitness of the multivariate model using the IL28B genotype was superior to that using the expression of hepatic ISGs. However, when these factors were included in the same model, the expression of hepatic ISGs was still useful for the predictive model independent of the IL28B genotype (Supplementary Table 6).

Table 3. Clinical Characteristics of 32 Patients Genotyped by GWAS and 5 SNPs in Strong Linkage Disequilibrium With IL28B,[11] Including rs12979860

Patient No.	Response	Age, y	Sex	F stage	ISGs	IL28B	RefSNP (chr pos) Minor allele	rs8105790 (44424341) C	rs11881222 (44426763) G	rs12979860 (44430627) T	rs8099917 (44435005) G	rs7248668 (44435661) A
1	SVR	42	M	1	4.20	83.8		TT	AA	CC	TT	GG
2	SVR	59	M	1	2.62	45.5		TT	AA	CC	TT	GG
3	SVR	41	F	1	1.54	1.3		TT	AA	CC	TT	GG
4	TR	57	M	1	3.18	21.7		TT	AA	CC	TT	GG
5	TR	68	F	1	1.43	20.3		TT	AA	CC	TT	GG
6	SVR	44	M	1	0.97	4.6		TT	AA	CC	TT	GG
7	SVR	61	M	2	2.15	6.1		TT	AA	CC	TT	GG
8	SVR	50	M	2	3.25	66.4		TT	AA	CC	TT	GG
9	SVR	49	M	2	1.25	ND		TT	AA	CC	TT	GG
10	TR	59	F	2	1.29	17.4		TT	AA	CC	TT	GG
11	SVR	48	F	2	1.00	90.2		TT	AA	CC	TT	GG
12	TR	65	F	2	2.86	36.4		TT	AA	CC	TT	GG
13	NR	34	M	3	0.82	17.8		TT	AA	CC	TT	GG
14	SVR	55	M	3	0.83	13.8		TT	AA	CC	TT	GG
15	TR	68	M	3	0.75	20.6		TT	AA	CC	TT	GG
16	SVR	64	M	3	0.94	15.7		TT	AA	CC	TT	GG
17	SVR	67	F	3	1.50	25.7		TT	AA	CC	TT	GG
18	SVR	48	M	4	1.69	7.9		TT	AA	CC	TT	GG
19	NR	66	F	1	4.57	16.5		TC	AG	CT	TG	GA
20	SVR	52	F	1	5.23	29.3		TC	AG	CT	TG	GA
21	NR	55	F	1	8.25	57.2		TC	AG	CT	TG	GA
22	SVR	49	F	1	5.36	ND		TC	AG	CT	TG	GA
23	TR	44	M	1	2.08	7.0		TC	AG	CT	TG	GA
24	NR	63	M	1	2.77	10.5		TC	AG	CT	TG	GA
25	NR	61	F	2	3.98	39.1		TC	AG	CT	TG	GA
26	NR	42	M	2	4.89	5.9		TC	AG	CT	TG	GA
27	SVR	49	M	3	3.31	6.9		TC	AG	CT	TG	GA
28	TR	71	F	3	5.53	27.3		TC	AG	CT	TG	GA
29	TR	63	M	3	3.40	33.5		TC	AG	CT	TG	GA
30	NR	70	F	3	4.78	8.1		TC	AG	CT	TG	GA
31	TR	62	F	3	3.53	14.0		TC	AG	CT	TG	GA
32	NR	56	M	4	7.37	30.8		CC	GG	TT	GG	AA

NOTE. The Pearson correlation of the r^2 estimates for adjacent pairs; rs8099917 vs rs8105790, rs8099917 vs rs11881222, rs8099917 vs rs12979860, and rs8099917 vs rs7248668 = 0.99, 0.99, 0.98, and 0.97, respectively.
IL28B, interleukin 28B; GWAS, genome-wide association studies; ISGs, interferon stimulated genes; SNP, single nucleotide polymorphism; SVR, sustained viral response; TR, transient response; NR, no response; M, male; F, female.

To examine further the different hepatic gene expression of patients with the major or minor genotypes, pathway analysis of differentially expressed genes between the 2 groups was performed. By comparing the expression of hepatic genes between patients with the major and minor genotypes, 1359 differentially expressed genes were identified ($P < .01$; 711 genes were up-regulated with the minor genotype, and 648 genes were up-regulated with the major genotype). Pathway analysis of these genes demonstrated that signaling pathways related to interferon action, apoptosis, and Wnt signaling were up-regulated in the liver of patients with the minor genotype, whereas B-cell-, dendritic cell-, and natural killer cell-related genes were up-regulated in the liver of patients with the major genotype (Supplementary Figure 3). These results suggest that IL28B may be involved in innate and adaptive immune responses and that different antiviral signaling pathways might be involved in the liver of patients with different SNPs.

Discussion

Multiple viral and host factors may be related to the treatment response to Peg-IFN and RBV combination therapy. For the viral factors, a higher number of aa substitutions in the ISDR of nonstructural 5A region was strongly associated with a favorable response to IFN-α monotherapy in patients with genotype-1 HCV.[4]

Besides viral factors, host factors such as age, gender, fibrotic stage of the liver, and the presence of steatosis and insulin resistance were associated with the treatment outcome.[20] Analysis of hepatic gene expression demonstrated that the up-regulation of ISGs in the liver before treatment may be related to a poor treatment response.[6-9] To reveal the underlying mechanism of treatment resistance, 2 reports compared gene expression profiling in the liver before and during therapy and showed that patients with up-regulated ISGs in the liver prior to treatment failed to further induce ISGs following the ad-

Table 4. Comparison of Clinical Factors Between Patients With Major (TT) and Minor (TG+GG) Alleles

Clinical category	TT		TG+GG		Univariate *P* value	Multivariate odds (95% CI)	Multivariate *P* value
No. of patients	n = 60		n = 31			—	
Treatment response							
SVR+TR vs NR	51 vs 9		11 vs 20		<.001	—	
Age and gender							
Age, *y*	56	(30–69)	56	(30–71)	.843	—	
Sex (M vs F)	39 vs 21		19 vs 12		.518	—	
Liver factors							
F stage (F1-2 vs F3-4)	36 vs 24		23 vs 17		.905	—	
A grade (A0-1 vs A2-3)	27 vs 33		20 vs 11		.075	—	
ISGs (Mx, IFI44, IFIT1) (<3.5 vs ≥3.5)	46 vs 14		5 vs 26		<.001	18.1 (3.95–113)	<.001
Laboratory parameters							
HCV-RNA (*KIU/mL*)	2055	(160–5000)	1970	(126–5000)	.602	—	
BMI (kg/m^2)	24.5	(16.3–40.5)	22.9	(19.1–26.6)	.006	—	.077
AST (*IU/L*)	59	(22–258)	54	(21–283)	.227	—	
ALT (*IU/L*)	75	(24–376)	60	(18–236)	.077	—	
γ-GTP (*IU/L*)	61	(4–392)	53	(20–229)	.517	—	.167
WBC ($/mm^3$)	4450	(2100–11,100)	4600	(2500–8200)	.947	—	
Hb (*g/dL*)	14.2	(11.4–16.7)	14.5	(11.2–17.2)	.606	—	
PLT ($\times 10^4/mm^3$)	15.4	(7–39.4)	16.2	(9.2–27.7)	.832	—	
TG (*mg/dL*)	98	(58–248)	131	(30–303)	.053	—	.055
T-Chol (*mg/dL*)	172	(115–222)	168	(129–237)	.910	—	
LDL-Chol (*mg/dL*)	84	(42–123)	69	(51–107)	.052	—	.055
HDL-Chol (*mg/dL*)	44	(18–72)	45	(29–77)	.218	—	
FBS (*mg/dL*)	95	(59–291)	96	(66–206)	.849	—	
Insulin (*μU/mL*)	7.5	(0.7–23.2)	9.2	(2–23.2)	.195	—	
HOMA-IR	1.3	(0.3–11.7)	1.2	(0.4–9.6)	.339	—	
Viral factors							
ISDR mutations (≤1 vs ≥2)	38 vs 22		23 vs 7		.194	—	.083
Treatment factors							
Total dose administrated							
Peg-IFN (μg)	3960	(1500–7200)	3840	(1920–5760)	.377	—	
RBV (*g*)	203	(26–336)	201	(106–268)	.777	—	
Achieved administration rate							
Peg-IFN (%)							
≥80%	41		17		.207	—	
<80%	19		14				
RBV (%)							
≥80%	34		19		.671	—	
<80%	26		12				
Achievement of EVR	40/60 (62%)		9/31 (29%)		<.001	—	

BMI, body mass index; AST, aspartate aminotransferase; ALT, alanine aminotransferase; IFI44, interferon-induced protein 44; IFIT1, interferon-induced protein with tetratricopeptide repeats 1; EVR, early virologic response; γ-GTP, γ-glutamyl transpeptidase; ISDR, interferon sensitivity determining region; Mx1, myxovirus (influenza virus) resistance 1 interferon-inducible protein p78 (mouse); WBC, leukocytes; HOMA-IR, homeostasis model assessment of insulin resistance; Hb, hemoglobin; RBV, ribavirin; PLT, platelets; TG, triglycerides; TR, transient response; T-chol, total cholesterol; LDL-chol, low-density lipoprotein cholesterol; HDL-chol, high-density lipoprotein cholesterol; FBS, fasting blood sugar; CI, confidence interval.

ministration of IFN and could not eliminate HCV.[6,7] We performed a similar analysis and observed that these findings were more evident in liver lobular cells than in infiltrating lymphocytes in the portal area (submitted for publication). Thus, both viral and host factors might be closely related to the treatment response to Peg-IFN and RBV combination therapy. However, the clinical relevance and relationships of these factors have not been fully evaluated. In this study, we validated the clinical significance of the expression of hepatic ISGs on treatment outcome using a relatively large cohort of patients and compared its significance with other viral and host factors. To compare the patients with SVR, TR, and NR, we assessed the overall plausibility of each group using Fisher C statistic,[16] and patients with SVR and TR were grouped together for further analysis.

We examined hepatic gene expression in 91 of 168 patients using the Affymetrix genechip. Expression profiling using 37 representative ISGs (see Materials and Methods), which were selected from gene expression profiling comparing pretreatment and under treatment liver, differentiated 2 groups of

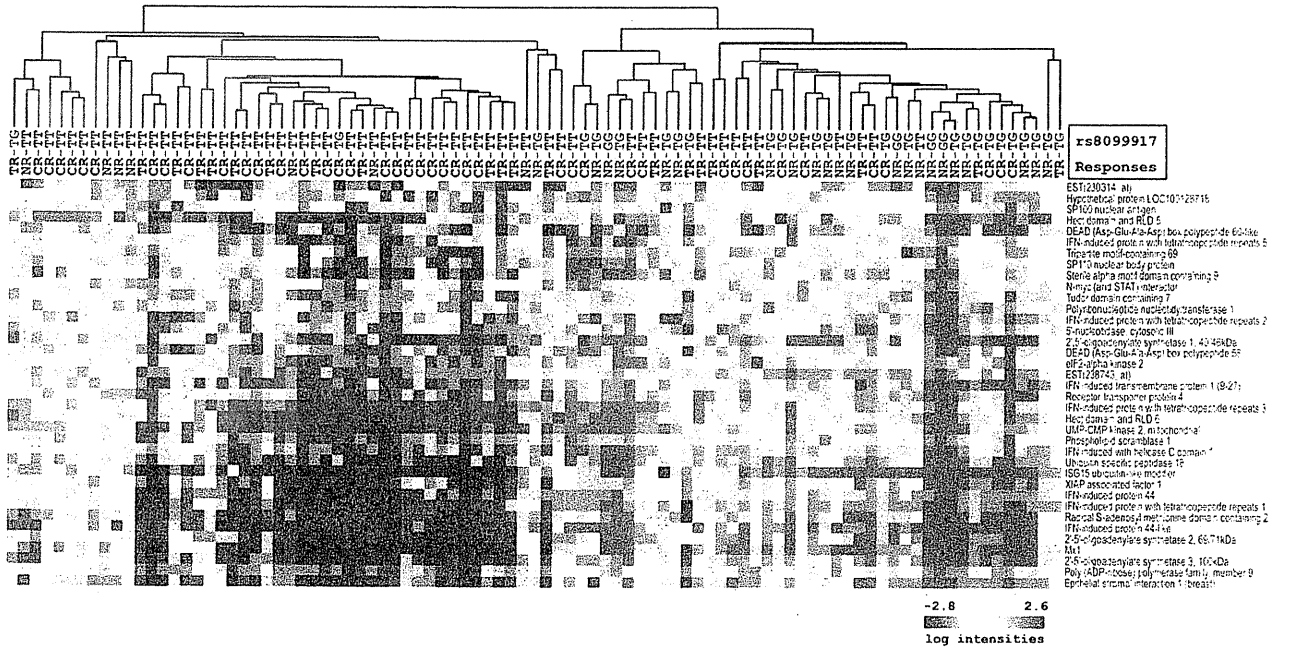

Figure 2. Hierarchical clustering analysis of 91 patients with the defined genotype of IL28B. Responses to therapy (SVR, TR, and NR) and IL28B genotype (TT, TG, or GG) are shown. The structure of the dendrogram and heat map is the same as in Figure 1.

patients: the Up-ISG and Down-ISG groups (Figure 1). The proportion of patients with NR to treatment was significantly higher in the Up-ISGs group.

Multivariate analysis showed that hepatic ISGs (<3.5), fibrosis stage (F1-F2), and ISDR mutations (≥2) significantly contributed to the outcome for the SVR+TR group (Table 1). Discriminate analysis using variables selected by multivariable analysis predicted the SVR+TR patients with 82% accuracy and NR patients with 79% accuracy. However, the accuracy decreased to 67% for SVR+TR patients and 53% for NR patients when the expression of hepatic ISGs was removed from the variables (data not shown). Interestingly, the expression of hepatic ISGs was strongly correlated with γ-GTP and weakly correlated with insulin resistance. A recent study describing the association between insulin resistance and poor treatment outcome might be partially explained by this observation.[20]

In this study, we utilized 3 ISGs (Mx1, IFI44, and IFIT1) out of 15 validated by RTD-PCR. The expression values of these ISGs were higher than those of other ISGs (Supplementary Figure 1*A*). We averaged these ISGs and set the cut-off value as 3.5 from the ROC curve (Supplementary Figure 1*B*). The sensitivity, specificity, and positive and negative predictive values on the likelihood of achieving SVR+TR using this cut-off value were 82% (103/125), 72% (31/43), 90% (103/115), and 58% (31/53), respectively. The results were compared with those observed for the 15 ISGs (Supplementary Table 5). These results showed that the 3.5 cut-off value for Mx1, IFI44, and IFIT1 would be valuable for clinical use.

Despite the importance of the expression of hepatic ISGs, viral factors may also allow us to predict the outcome of treatment. Multivariate analysis showed that ISDR mutations (≥2) independently contributed to the treatment outcome, although univariate analysis did not show significance (P = .07); therefore, ISDR might be uniquely and differentially involved in treatment resistance.

What causes the differences in the expression of hepatic ISGs? In parallel to the gene expression analysis, a GWAS was applied to identify genomic loci associated with treatment response, and a polymorphism in IL28B was found to predict hepatitis C treatment-induced viral clearance.[10-12] To examine the relationship between the genetic variation of IL28B and hepatic gene expression, we determined the IL28B polymorphism in 91 patents (Table 3). The patients with the minor genotype (TG or GG) had an increased expression of hepatic ISGs compared with the patients with major genotype (TT) (Figures 2 and 3). In European-Americans, the proportion of major homozygotes is 39% (CC at rs1297986), 49% for heterozygotes (TC), and 12% for minor homozygotes (TT).[11] Although the proportion of minor homozygotes was much less in this study (GG, 4%), as reported in a previous study in Japan,[12] more patients are required for proper evaluation. It is interesting that the expression of hepatic ISGs in minor homozygotes (GG) was higher than in heterozygotes (TG) in this study.

The results clearly showed that the differences in the expression of hepatic ISGs before treatment are associated with the IL28B polymorphism and results in different treatment outcomes. Although we could not detect significant differences in the expression levels of IL28B depending on the different SNP, some patients with the major genotype showed a higher expression of IL28B. Because IL28B expression was approximately 10-fold less than the expression of ISGs, the lower

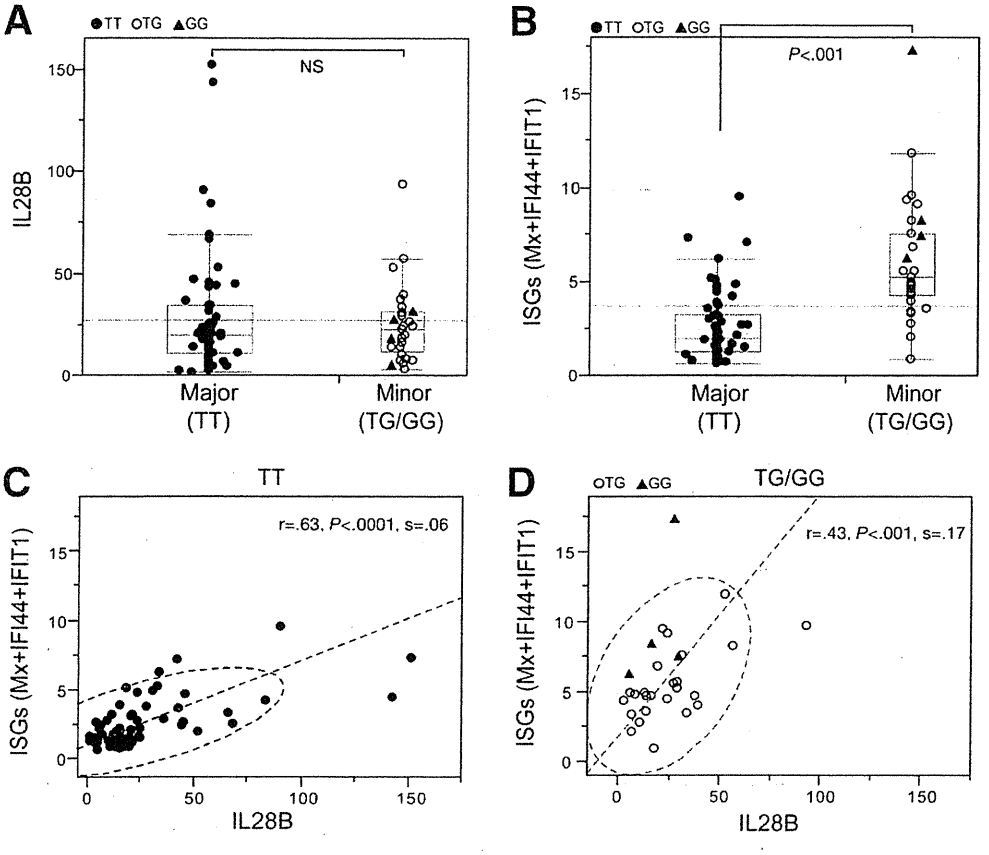

Figure 3. (*A*) IL28 expression in the liver of 91 patients with the major (TT) or minor (TG or GG) genotype (rs8099917). (*B*) Expression of ISGs in the liver of patients with the major (TT) or minor (TG or GG) genotype (rs8099917). (*C*) Relationship between IL28 and ISGs in the liver of patients with the major (TT) genotype (rs8099917). (*D*) Relationship between IL28 and ISGs in the liver of patients with the minor (TG or GG) genotype (rs8099917).

expression of IL28B may be a reason for the decreased ability to distinguish differences in its expression. Another possibility may be the specificity of the IL28B primers used in this study; because IL28B shares a 98.2% nucleotide sequence homology with IL28A, IL28B specific primers are not available.[21] When the expression of IL28B and hepatic ISGs were compared, a significant correlation was observed, and, interestingly, IL28B and ISGs derived from different SNPs were correlated in a different way (Figure 3*C* and *D*). It appeared that hepatic ISGs were more induced by the reduced amounts of IL28B in patients with the minor genotype. The mechanism behind these findings has yet to be determined; however, IL28B interacts with a heterodimeric class II cytokine receptor that consists of IL-10 receptor β (IL-10Rβ) and IL-28 receptor α (IL-28Rα).[18,19] It is possible that IL28B could mediate antiviral signaling through IL-10 signaling as well as STAT1 activation. The Th 2 dominant signaling of IL28B may modulate signaling pathways in livers with CH-C and contributes to the different expression of ISGs. Another possibility may be that the cell origin of hepatic ISGs is different. A recent study revealed cell-type specific ISG expression in macrophages and hepatocytes, which could be related to the IFN response.[22] As more of the B-cell-, dendritic cell-, and natural killer cell-related genes were up-regulated in the liver of patients with the major genotype, ISGs could be expressed by these cells, whereas they are expressed by hepatocytes in the liver of patients with the minor genotype. It is known that the induction of ISGs in lymphocytes is lower than that in hepatocytes. The precise mechanism should be investigated further as a different regulatory mechanism for the expression of ISGs may be present.

In conclusion, we presented the clinical relevance of the expression of hepatic ISGs for the treatment outcome of Peg-IFN and RBV combination therapy. The different expressions of hepatic ISGs before treatment might be due to polymorphisms in IL28B. Further studies are required to clarify the detailed pathways of IL28B and hepatic gene expression through molecular biologic and immunologic aspects.

Supplementary Material

Note: To access the supplementary material accompanying this article, visit the online version of *Gastroenterology* at www.gastrojournal.org, and at doi: 10.1053/j.gastro.2010.04.049.

Appendix 1. The Hokuriku Liver Study Group (HLSG) is Composed of the Following Members:

Drs Takashi Kagaya, Kuniaki Arai, Kaheita Kakinoki, Kazunori Kawaguchi, Hajime Takatori, Hajime Sunakosaka (Department of Gastroenterology, Kanazawa University Graduate School of Medicine, Kanazawa); Drs Touru

Nakahama, Shinji Kamiyamamoto (Kurobe City Hospital, Kurobe, Toyama); Dr Yasuhiro Takemori (Toyama Rosai Hospital, Uozu, Toyama); Dr Hikaru Oguri (Koseiren Namerikawa Hospital, Namerikawa, Toyama); Drs Yatsugi Noda, Hidero Ogino (Toyama Prefectural Central Hospital, Toyama, Toyama); Drs Yoshinobu Hinoue, Keiji Minouchi (Toyama City Hospital, Toyama, Toyama); Dr Nobuyuki Hirai (Koseiren Takaoka Hospital, Takaoka, Toyama); Drs Tatsuho Sugimoto, Koji Adachi (Tonami General Hospital, Tonami, Toyama); Dr Yuichi Nakamura (Noto General Hospital, Nanao, Ishikawa); Drs Masashi Unoura, Ryuhei Nishino (Public Hakui Hospital, Hakui, Ishikawa); Drs Hideo Morimoto, Hajime Ohta (National Hospital Organization Kanazawa Medical Center, Kanazawa, Ishikawa); Dr Hirokazu Tsuji (Kanazawa Municipal Hospital, Kanazawa, Ishikawa); Drs Akira Iwata, Shuichi Terasaki (Kanazawa Red Cross Hospital, Kanazawa, Ishikawa); Drs Tokio Wakabayashi, Yukihiro Shirota (Saiseikai Kanazawa Hospital, Kanazawa, Ishikawa); Drs Takeshi Urabe, Hiroshi Kawai (Public Central Hospital of Matto Ishikawa, Hakusan, Ishikawa); Dr Yasutsugu Mizuno (Nomi Municipal Hospital, Nomi, Ishikawa); Dr Shoni Kameda (Komatsu Municipal Hospital, Komatsu, Ishikawa); Drs Hirotoshi Miyamori, Uichiro Fuchizaki (Keiju Medical Center, Nanao, Ishikawa); Dr Haruhiko Shyugo (Kanazawa Arimatsu Hospital, Kanazawa, Ishikawa); Dr Hideki Osaka (Yawata Medical Center, Komatsu, Ishikawa); Dr Eiki Matsushita (Kahoku Central Hospital, Tsubata, Ishikawa); Dr Yasuhiro Katou (Katou Hospital, Komatsu, Ishikawa); Drs Nobuyoshi Tanaka, Kazuo Notsumata (Fukuiken Saiseikai Hospital, Fukuil, Fukui); Dr Mikio Kumagai (Kumagai Clinic, Tsuruga, Fukui); Dr Manabu Yoneshima (Municipal Tsuruga Hospital, Tsuruga, Fukui).

References

1. Kiyosawa K, Sodeyama T, Tanaka E, et al. Interrelationship of blood transfusion, non-A, non-B hepatitis and hepatocellular carcinoma: analysis by detection of antibody to hepatitis C virus. Hepatology 1990;12:671–675.
2. Fried MW, Shiffman ML, Reddy KR, et al. Peginterferon alfa-2a plus ribavirin for chronic hepatitis C virus infection. N Engl J Med 2002;347:975–982.
3. Poynard T, Ratziu V, McHutchison J, et al. Effect of treatment with peginterferon or interferon alfa-2b and ribavirin on steatosis in patients infected with hepatitis C. Hepatology 2003;38:75–85.
4. Enomoto N, Sakuma I, Asahina Y, et al. Mutations in the nonstructural protein 5A gene and response to interferon in patients with chronic hepatitis C virus 1b infection. N Engl J Med 1996; 334:77–81.
5. Okanoue T, Itoh Y, Hashimoto H, et al. Predictive values of amino acid sequences of the core and NS5A regions in antiviral therapy for hepatitis C: a Japanese multi-center study. J Gastroenterol 2009;44:952–963.
6. Feld JJ, Nanda S, Huang Y, et al. Hepatic gene expression during treatment with peginterferon and ribavirin: identifying molecular pathways for treatment response. Hepatology 2007;46:1548–1563.
7. Sarasin-Filipowicz M, Oakeley EJ, Duong FH, et al. Interferon signaling and treatment outcome in chronic hepatitis C. Proc Natl Acad Sci U S A 2008;105:7034–7039.
8. Asselah T, Bieche I, Narguet S, et al. Liver gene expression signature to predict response to pegylated interferon plus ribavirin combination therapy in patients with chronic hepatitis C. Gut 2008;57:516–524.
9. Chen L, Borozan I, Feld J, et al. Hepatic gene expression discriminates responders and nonresponders in treatment of chronic hepatitis C viral infection. Gastroenterology 2005;128:1437–1444.
10. Thomas DL, Thio CL, Martin MP, et al. Genetic variation in IL28B and spontaneous clearance of hepatitis C virus. Nature 2009; 461:798–801.
11. Ge D, Fellay J, Thompson AJ, et al. Genetic variation in IL28B predicts hepatitis C treatment-induced viral clearance. Nature 2009;461:399–401.
12. Tanaka Y, Nishida N, Sugiyama M, et al. Genome-wide association of IL28B with response to pegylated interferon-α and ribavirin therapy for chronic hepatitis C. Nat Genet 2009;41:1105–1109.
13. Desmet VJ, Gerber M, Hoofnagle JH, et al. Classification of chronic hepatitis: diagnosis, grading and staging. Hepatology 1994;19:1513–1520.
14. Honda M, Yamashita T, Ueda T, et al. Different signaling pathways in the livers of patients with chronic hepatitis B or chronic hepatitis C. Hepatology 2006;44:1122–1138.
15. Honda M, Kaneko S, Kawai H, et al. Differential gene expression between chronic hepatitis B and C hepatic lesion. Gastroenterology 2001;120:955–966.
16. Shipley B. A new inferential test for path models based on directed acyclic graphs. Structural Equation Modeling 2000;7:206–218.
17. Favre M, Martin J, Festa-Bianchet M. Determinants and life-history consequences of social dominance in bighorn ewes. Anim Behav 2008;76:1373–1380.
18. Sheppard P, Kindsvogel W, Xu W, et al. IL-28, IL-29, and their class II cytokine receptor IL-28R. Nat Immunol 2003;4:63–68.
19. Kotenko SV, Gallagher G, Baurin VV, et al. IFN-λ mediate antiviral protection through a distinct class II cytokine receptor complex. Nat Immunol 2003;4:69–77.
20. Camma C, Bruno S, Di Marco V, et al. Insulin resistance is associated with steatosis in nondiabetic patients with genotype 1 chronic hepatitis C. Hepatology 2006;43:64–71.
21. Mihm S, Frese M, Meier V, et al. Interferon type I gene expression in chronic hepatitis C. Lab Invest 2004;84:1148–1159.
22. Chen L, Borozan I, Sun J, et al. Cell-type specific gene expression signature in liver underlies response to interferon therapy in chronic hepatitis C infection. Gastroenterology 2010;138:942–948.

Received October 9, 2009. Accepted April 14, 2010.

Reprint requests

Address requests for reprints to: Shuchi kaneko, MD, PhD, Department of Gastroenterology, Graduate School of Medicine, Kanazawa University, Takara-Machi 13-1, Kanazawa 920-8641, Japan. e-mail: skaneko@m-kanazawa.jp; fax: (81) 76-234-4250.

Acknowledgments

The authors thank Nami Nishiyama and Yuki Hatayama for excellent technical assistance.

Participating investigators are listed in Appendix 1.

Conflicts of interest

The authors disclose no conflicts.

Funding

This work was supported in part by a grant-in-aid from the Ministry of Health, Labour and Welfare of Japan.

Differential MicroRNA Expression Between Hepatitis B and Hepatitis C Leading Disease Progression to Hepatocellular Carcinoma

Shunsuke Ura,[1] Masao Honda,[1,2] Taro Yamashita,[1] Teruyuki Ueda,[1] Hajime Takatori,[1] Ryuhei Nishino,[1] Hajime Sunakozaka,[1] Yoshio Sakai,[1] Katsuhisa Horimoto,[3] and Shuichi Kaneko[1]

MicroRNA (miRNA) plays an important role in the pathology of various diseases, including infection and cancer. Using real-time polymerase chain reaction, we measured the expression of 188 miRNAs in liver tissues obtained from 12 patients with hepatitis B virus (HBV)-related hepatocellular carcinoma (HCC) and 14 patients with hepatitis C virus (HCV)-related HCC, including background liver tissues and normal liver tissues obtained from nine patients. Global gene expression in the same tissues was analyzed via complementary DNA microarray to examine whether the differentially expressed miRNAs could regulate their target genes. Detailed analysis of the differentially expressed miRNA revealed two types of miRNA, one associated with HBV and HCV infections (n = 19), the other with the stage of liver disease (n = 31). Pathway analysis of targeted genes using infection-associated miRNAs revealed that the pathways related to cell death, DNA damage, recombination, and signal transduction were activated in HBV-infected liver, and those related to immune response, antigen presentation, cell cycle, proteasome, and lipid metabolism were activated in HCV-infected liver. The differences in the expression of infection-associated miRNAs in the liver correlated significantly with those observed in Huh7.5 cells in which infectious HBV or HCV clones replicated. Out of the 31 miRNAs associated with disease state, 17 were down-regulated in HCC, which up-regulated cancer-associated pathways such as cell cycle, adhesion, proteolysis, transcription, and translation; 6 miRNAs were up-regulated in HCC, which down-regulated anti-tumor immune response. *Conclusion:* miRNAs are important mediators of HBV and HCV infection as well as liver disease progression, and therefore could be potential therapeutic target molecules. (HEPATOLOGY 2009;49:1098-1112.)

MicroRNA (miRNA) is an endogenous, small, single-strand, noncording RNA consisting of 20 to 25 bases and regulates gene expression of various cell types. It plays an important role in various biological processes, including organ development and differentiation as well as cellular death and proliferation, and is also involved in various diseases such as infection and cancer.[1-3]

miRNAs are produced as follows. A primary miRNA with a hairpin loop structure is cleaved into a precursor miRNA and transported out of the nuclei with a carrier protein (Exportin-5). The precursor miRNA is then processed by Dicer and converted into an active single-strand RNA in the cytoplasm. The miRNA binds to a target messenger RNA in a sequence-dependent manner and induces degradation of the target messenger RNA and translational inhibition. One miRNA regulates the expression of multiple target genes; bioinformatics analyses have suggested that the expression of more than 30% of human genes is regulated by miRNAs.[4-7]

Abbreviations: cDNA, complementary DNA; CH, chronic hepatitis; CH-B, chronic hepatitis B; CH-C, chronic hepatitis C; HBV, hepatitis B virus; HCC, hepatocellular carcinoma; HCC-B, hepatitis B-related hepatocellular carcinoma; HCC-C, hepatitis C-related hepatocellular carcinoma; HCV, hepatitis C virus; miRNA, microRNA; RTD-PCR, real-time detection polymerase chain reaction; SVM, support vector machine.

From the Departments of [1]Gastroenterology and [2]Advanced Medical Technology, Kanazawa University Graduate School of Medicine, Kanazawa, Japan; and the [3]Biological Network Team, Computational Biology Research Center, National Institute of Advanced Industrial Science and Technology, 2-42 Aomi, koto-ku, Tokyo 135-0064, Japan.

Received July 3, 2008; accepted November 15, 2008.

Address reprint requests to: Masao Honda, M.D., Ph.D., Department of Gastroenterology, Graduate School of Medicine, Kanazawa University, Takara-Machi 13-1, Kanazawa 920-8641, Japan. E-mail: mhonda@m-kanazawa.jp; fax: (81)-76-234-4250.

Published online in Wiley InterScience (www.interscience.wiley.com).

DOI 10.1002/hep.22749

Potential conflict of interest: Nothing to report.

Additional Supporting Information may be found in the online version of this article.

Table 1. Characteristics of Patients Used for Analysis of miRNA and Microarray Samples

Patient No.	Virus	Age	Sex	ALT	Histology of Activity	Background Liver Fibrosis	Histological Grade of HCC	Tumor Size (mm)	TNM Staging	HCV-RNA (KIU/mL)	HBV-DNA (LEG/mL)
1	HBV	57	M	16	2	4	Moderate	20	II	–	3.4
2	HBV	51	M	57	1	2	Moderate	48	II	–	< 2.6
3	HBV	61	M	17	1	4	Well	16	II	–	< 3.7
4	HBV	47	M	19	1	4	Moderate	15	I	–	< 3.7
5	HBV	72	M	19	1	1	Well	25	II	–	NA
6	HBV	73	M	62	1	3	Moderate	45	III	–	5.7
7	HBV	42	M	36	1	4	Moderate	18	I	–	< 3.7
8	HBV	63	M	13	1	2	Moderate	15	I	–	2.8
9	HBV	68	F	54	1	2	Well	56	II	–	4.1
10	HBV	70	M	13	0	2	Well	40	II	–	< 3.7
11	HBV	58	M	29	1	4	Moderate	35	IVA*	–	3.3
12	HBV	72	M	22	1	4	Moderate	18	I	–	6
13	HCV	66	F	33	2	4	Well	25	II	423	–
14	HCV	67	M	89	1	4	Well	30	II	> 850	–
15	HCV	64	M	31	1	4	Moderate	75	III	< 5 (+)	–
16	HCV	68	M	30	0	4	Well	23	II	> 850	–
17	HCV	46	M	98	2	3	Moderate	20	I	> 850	–
18	HCV	68	F	32	2	4	Moderate	25	III	< 5 (+)	–
19	HCV	66	F	46	2	4	Well	25	II	> 850	–
20	HCV	47	M	246	1	3	Moderate	20	I	262	–
21	HCV	75	M	27	1	3	Moderate	19	II	85.1	–
22	HCV	77	M	21	0	1	Moderate	20	II	< 5 (−)	–
23	HCV	66	M	46	2	2	Well	60	II	50.3	–
24	HCV	65	M	89	1	1	Poorly	25	III	850	–
25	HCV	53	M	54	0	1	Moderate	28	II	< 5 (−)	–
26	HCV	75	F	212	1	4	Well	19	I	580	–
27	–	51	F	18	0	0	–	–	–	–	–
28	–	78	F	13	0	0	–	–	–	–	–
29	–	75	M	20	0	0	–	–	–	–	–
30	–	34	M	12	0	0	–	–	–	–	–
31	–	64	M	30	0	0	–	–	–	–	–
32	–	78	M	9	0	0	–	–	–	–	–
33	–	53	M	19	0	0	–	–	–	–	–
34	–	64	F	12	0	0	–	–	–	–	–
35	–	60	F	20	0	0	–	–	–	–	–

HCV RNA was assayed via Amplicor Monitor Test (KIU/mL); HBV DNA was assayed via transcription-mediated amplification (LEG/mL).

Abbreviations: ALT, alanine aminotransferase; F, female; HBV, hepatitis B virus; HCC, hepatocellular carcinoma; HCV, hepatitis C virus; M, male; TNM, tumor-node–metastasis.

*Vascular invasion (+).

Infection of the human liver with hepatitis B virus (HBV) and hepatitis C virus (HCV) induces the development of chronic hepatitis (CH), cirrhosis, and in some instances hepatocellular carcinoma (HCC).[8] The virological features of these two distinct viruses are completely different; however, the viruses infect the liver and cause CH, which is not distinguished by histological examination or clinical manifestations. We previously reported that gene expression profiles in chronic hepatitis B (CH-B) and chronic hepatitis C (CH-C) are different. Proapoptotic and DNA repair responses were predominant in CH-B, and inflammatory and antiapoptotic phenotypes were predominant in CH-C. However, factors inducing these differences in gene expression remain to be elucidated.[9,10]

We examined miRNA expression in liver tissue with HBV-related liver disease (CH-B and HCC-B) and HCV-related liver disease (CH-C and HCC-C) and in normal liver tissue via real-time detection polymerase chain reaction (RTD-PCR). We also performed global analysis of messenger RNA expression in these tissues using complementary DNA (cDNA) microarray. These analyses allowed us to find characteristic miRNAs associated with HBV or HCV infection as well as the progression of liver disease.

Patients and Methods

Patients. The study subjects included 12 patients with CH-B complicated by HCC and 14 patients with

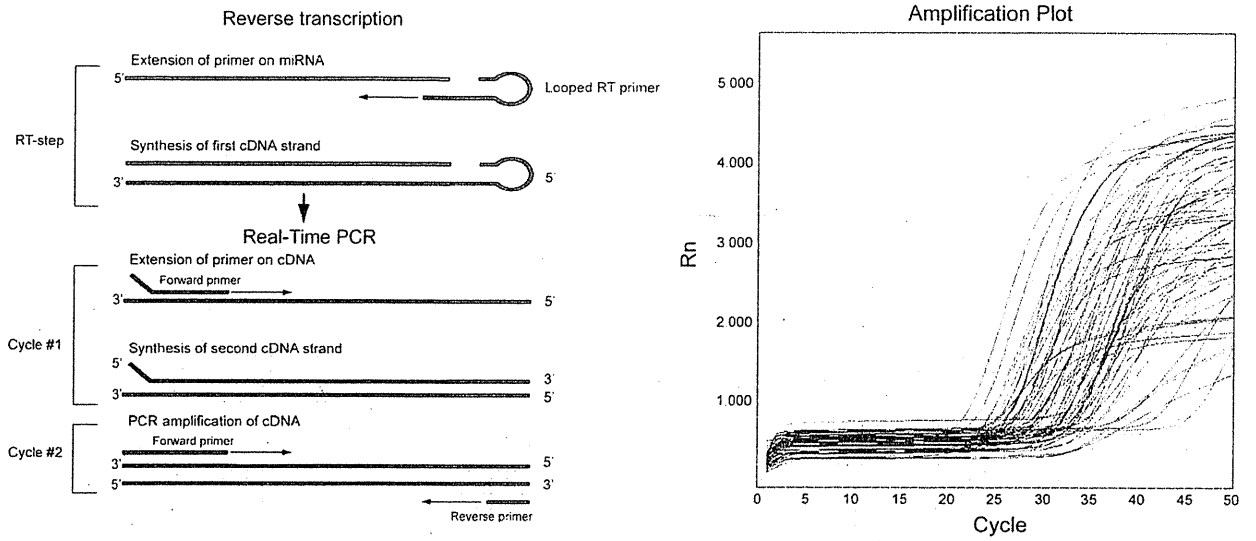

Fig. 1. (A) miRNA-specific RTD-PCR using sheet hairpin primers. (B) miRNA amplification curves by RTD-PCR.

CH-C complicated by HCC. Gene expression analysis was approved by the ethics committee of the Graduate School of Medicine, Kanazawa University Hospital, Japan, between 1999 and 2004. In addition, nine normal liver tissue samples obtained during surgery for metastatic liver cancer were used as control samples. Surgically removed liver tissues were stored in liquid nitrogen until analysis. Histological classification of HCC and histological evaluation of hepatitis in noncancerous regions for each patient are shown in Table 1. HCV viremia in two patients with CH-C was persistently cleared by interferon therapy before HCC development. There were no significant differences in the histological findings of HCC and noncancerous regions, as well as in sex, age, and hepatic function between the HBV and HCV infection groups.

Quantitative RTD-PCR. Approximately 1 mg of each liver tissue sample stored in liquid nitrogen was ground with a homogenizer while still frozen, and total RNA containing miRNA was isolated according to the protocol of the mirVana miRNA Isolation kit (Ambion, Austin, TX) and stored at −80°C until analysis. miRNA expression levels were quantitated using the TaqMan MicroRNA Assays Human Panel Early Access kit (Applied Biosystems, Foster City, CA). cDNA was prepared via reverse transcription using 10 ng each of the isolated total RNA and 3 μL each of the reverse transcription primers with specific loop structures. Reverse transcription was performed using the TaqMan MicroRNA Reverse Transcription kit (Applied Biosystems) according to the manufacturer's protocol. Then, a mixture of 6.67 μL of nuclease-free water, 10 μL of TaqMan 2 × Universal PCR Master Mix (No AmpErase UNG; Applied Biosystems), and 2 μL of TaqMan MicroRNA Assay Mix, which was included in the kit, was prepared for each sample on a 384-well plate; 1.33 μL of the reverse transcription product was added to the mixture, and amplification reaction was performed on an ABI PRISM 7900HT (Applied Biosystems). Expression levels of 188 miRNAs in each sample were quantitated.

Analysis of RTD-PCR Data. The measured 188 miRNAs included RNU6B, which is commonly used as a control for miRNA. β-Actin and glyceraldehyde 3-phosphate dehydrogenase were also measured simultaneously for correcting RNA amount. The mean Ct values and standard deviations of each miRNA were calculated from expression data of all patients obtained by RTD-PCR. miRNA with the lowest expression variation was used as the internal control. Ct values of each miRNA were then corrected by the Ct value of the internal control to yield −ΔCt values defined as relative miRNA expression levels and used for analyses. Statistical analyses and hierarchical cluster analyses of expression data were performed using BRB ArrayTools (http://linus.nci.nih.gov/BRB-ArrayTools.html). Relative miRNA expression levels were further normalized using the median over the all patients so that the normalized expression levels of each patient have a median log ratio of 0. A class prediction method was used for classifying two patient groups based on the supervised learning method, and a binary tree classification method was used for classifying three or more patient groups with a statistical algorithm of the support vector machine (SVM). Class prediction was performed using SVM incorporating genes differentially expressed at a univariate parametric significance level of $P = 0.01$. The prediction rate was estimated via cross-validation and the bootstrap method for small sample data.[11] (It is worth

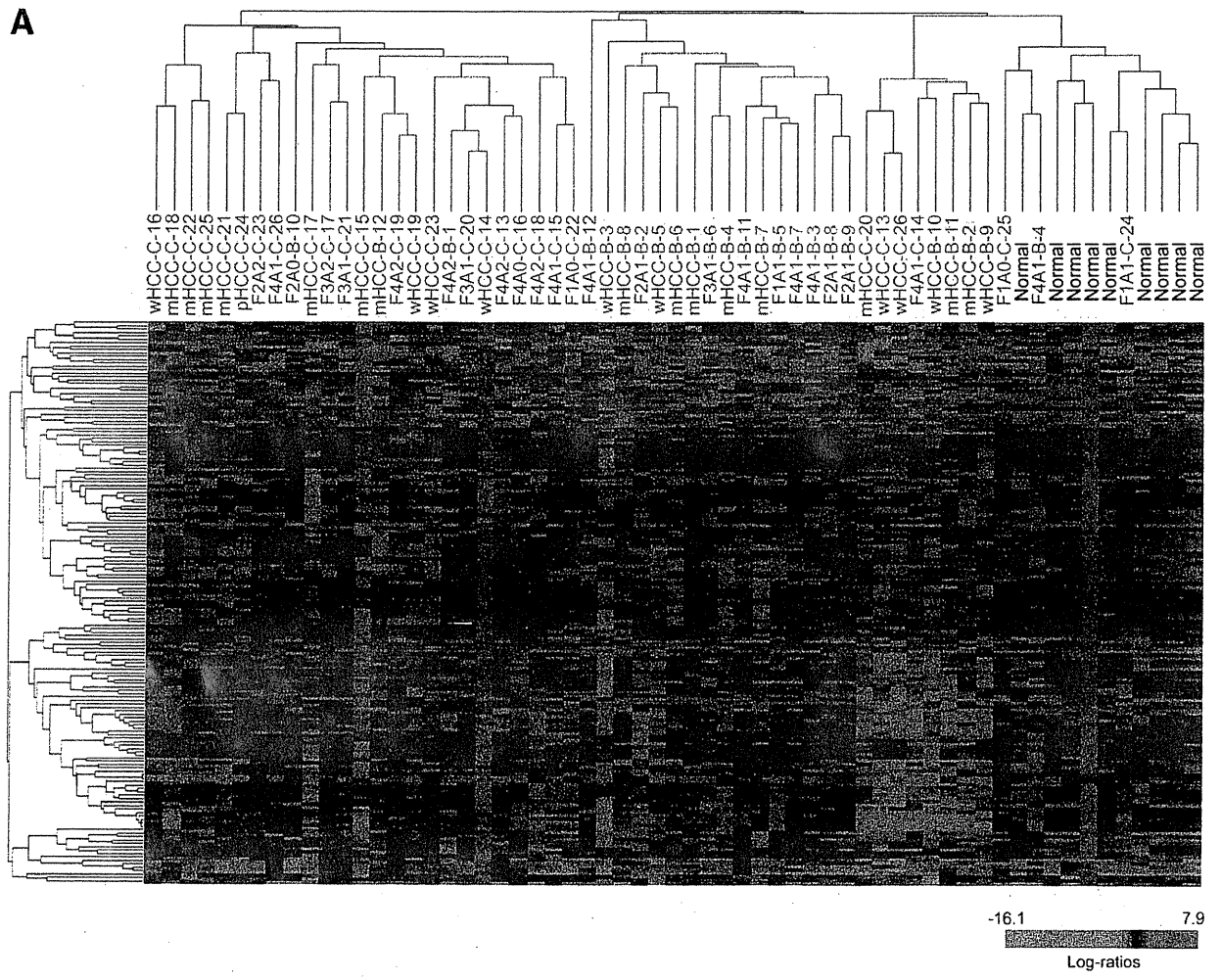

Fig. 2. (A) Hierarchical cluster analysis using total miRNA. Chronic hepatitis is indicated by histological stage and grade (F, fibrosis; A, activity) and type of infecting virus (B or C). HCC is indicated by histological grade (w, well differentiated; m, moderately differentiated; p, poorly differentiated) and type of infecting virus (B or C), with the patient number added at the end. (B) Relationship between five classes divided by binary tree classification. Expression profiles were first classified into normal liver and non-normal liver groups (node 1), then into HBV and HCV groups (node 2). The HBV group was further divided into HCC-B and CH-B (node 3), and the HCV group into HCC-C and CH-C (node 4).

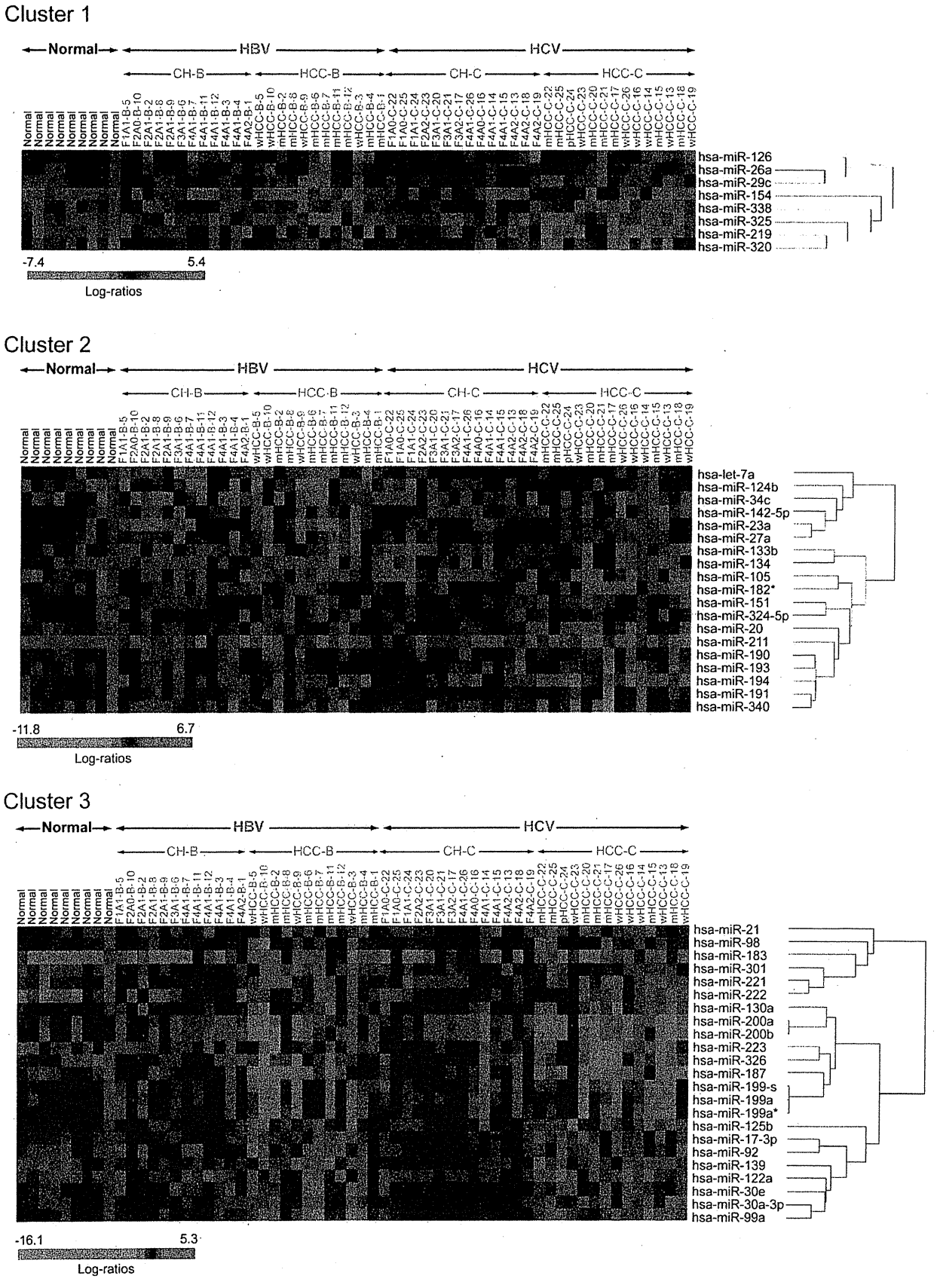

Fig. 3. Cluster 1: Eight miRNAs specifically differentiated node 1 classification. Cluster 2: Nineteen miRNAs specifically differentiated node 2 classification. Cluster 3: Twenty-three miRNAs differentiated CH-B and HCC-B as well as CH-C and HCC-C.

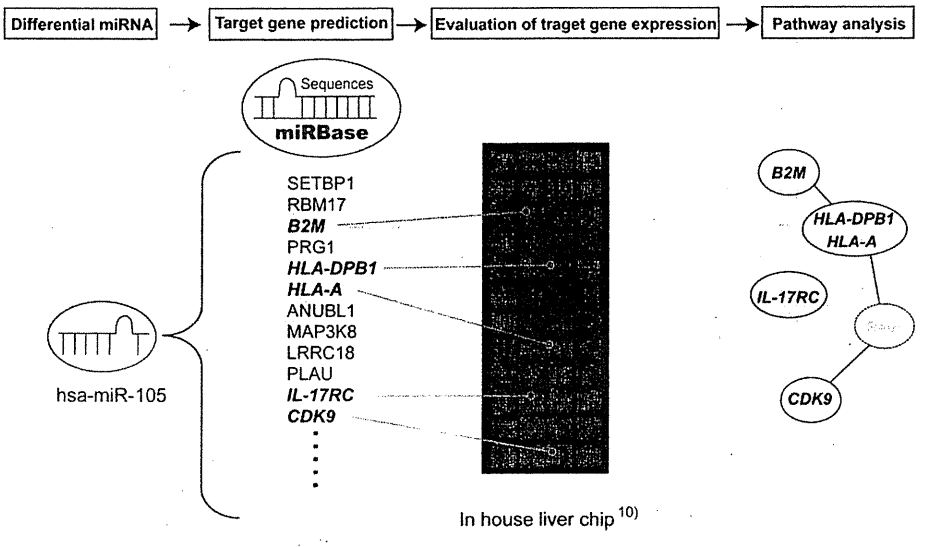

Fig. 4. Analysis of miRNA expression data. Target genes of miRNAs were predicted using MIRANDA Pro3.0; candidate target genes spotted on microarray were identified; number of genes that actually exhibit significant ($P < 0.05$) changes in expression among the genes was determined; and signal pathways involving genes regulated by the miRNAs that had exhibited differential expression between each group were analyzed using MetaCore (Table 4).

noting that the prediction rate may be likely an overestimate of the true rate, given the weaknesses of cross-validation and bootstrapping methods in a strict sense.)

Microarray Analysis. cDNA microarray slides (Liver chip 10k) were used as described.[10] RNA isolation, amplification of antisense RNA, labeling, and hybridization were performed according to the protocols described.[9,10] Quantitative assessment of the signals on the slides was performed by scanning on the ScanArray 5000 (General Scanning, Watertown, MA) followed by image analysis using GenePix Pro 4.1 (Axon Instruments, Union City, CA) as described.[10]

Preliminary Survey of Independency of Paired Samples from the Same Patient. CH and HCC expression data were derived from the same patient. Before further analysis, we examined whether the miRNA expression of paired samples was similar or independent. We compared differences in the expressions of paired and nonpaired CH and HCC samples using the Dunnett test[12] (Supplementary Data). All possible tests performed for data pairs represented no dependency due to the paired data from the same patients. For data analysis, we used the standard pairwise class comparison and prediction tool in BRB ArrayTools.

Identification of Candidate miRNA Target Genes. Candidate target genes predicted to be regulated by miRNAs based on sequence comparison were selected using MIRANDA Pro3.0 (Sanger Institute). Of the selected genes, those represented on a microarray chip were then examined for expression (Fig. 4). The number of genes showing a significant ($P < 0.05$) expression difference among the candidate target genes represented on the chip was statistically analyzed to evaluate the significance of expression regulation by miRNAs. Analysis of significance was performed using Hotelling T2 test (BRB ArrayTools).

Pathway Analysis. Of the candidate miRNA target genes, those showing a significant ($P < 0.01$) expression difference between N, CH-B, HCC-B, CH-C, and HCC-C samples were analyzed for pathways involving these genes using MetaCore software suite (GeneGo, St. Joseph, MI). Significance probability was calculated using

Table 2-1. Class Prediction

No.	Class	Prediction (%)	No. of Predictors	*P* Value
1	HBV versus HCV	87	32	<0.001
2	N versus CH (B+C)	91	26	0.007
3	CH (B+C) versus HCC (B+C)	92	34	0.003

Class prediction algorithm was used for the classification of two groups of patients. Feature selection was based on the univariate significance level (alpha = 0.01). The support vector machine classifier was used for class prediction.

Abbreviations: CH, nontumor lesion of HCC; HCC, hepatocellular carcinoma; N, normal.

Table 2-2 Binary Tree Classification

Node	Group 1 Class	Group 2 Class	No. of Predictors	Misclassification Rate (%)
1	HCC-B, HCC-C, CH-B, CH-C	N	20	4.9
2	HCC-B, CH-B	HCC-C, CH-C	19	13.5
3	HCC-B	CH-B	15	29.2
4	HCC-C	CH-C	14	17.9

Binary tree classification algorithm was used for the classification of each category of patients. Feature selection was based on the univariate significance level (alpha = 0.01). The support vector machine classifier was used for class prediction. There were four nodes in the classfication tree.

Abbreviations: CH-B, non-tumor lesion of HCC-B; CH-C, nontumor lesion of HCC-C; HCC-B, hepatitis B virus-related hepatocellular carcinoma; HCC-C, hepatitis C virus-related hepatocellular carcinoma; N, normal

Table 3-1. Representative miRNAs That Were Commonly Repressed in CH-B, CH-C, HCC-B, and HCC-C Compared with Normal Liver (Cluster)

miRNA	Parametric *P* Value	Ratio*	No. of Significant Genes/Predicted Target Genes†	Hotelling Test *P* Value‡	Differentially Expressed Target Genes§	Pathway of Regulated Genes¶
hsa-miR-219	7.3E-05	0.28	25/109	2.59E-04	Glypican-3, ERP5, PLK2, HIRA, HMG2	Regulatory T cell differentiation
					ACOX1	Fatty acid beta-oxidation
					NF-X1	MHC class II biosynthetic process
hsa-miR-320	9.8E-05	0.50	26/88	3.50E-06	Vimentin, ALP (*N*-acetyltransferase-like), SEC61 beta, G-protein alpha-i2, Filamin A	Protein kinase cascade
					Rac1, RhoG	Organelle organization and biogenesis
					Vinexin beta, Profilin I, Ca-ATPase3	Actin cytoskeleton organization and biogenesis
hsa-miR-154	2.7E-04	0.15	22/70	5.40E-06	OTR, NET1(TSPAN1), NAP1, Vimentin, PDIA3, cytochrome P-450 reductase	Regulation of apoptosis
					DLX2	Morphogenesis
					GUAC, ACAT1	Branched chain family amino acid catabolic process
hsa-miR-29c	1.8E-03	0.55	53/133	1.00E-06	FBXO7, ASPP1, HSPA4, Cathepsin O, PDF, COL4A1, HSPA4, TIP30, CXADR	Cell-substrate adhesion
					NS1-BP, ALP (*N*-acetyltransferase-like), ACTR10, Beclin 1	Transcription, DNA-dependent
					SMAD6, LTBR(TNFRSF3), ENPP7	Apoptosis
hsa-miR-338	5.2E-03	0.46	30/101	3.60E-06	ID3, GATA-4, NFIA, FR-beta, CREST, HYOU1	Developmental process
					G3ST1, CAD,	Immune effector process
					FKBP12, LZIP, PDIA3, Schwannomin (NF2), CREST	Immune system process
hsa-miR-26a	6.3E-03	0.70	37/119	2.64E-05	*LIG4*, c-FLIP, GADD45 beta, DAPK1, PRDX4, LRP130	Response to stimulus
					Cyclin E, ZDHHC6, Tx1, ATG8 (GATE-16), WASP, C1s	DNA replication initiation
					COPG1	Ion transport
hsa-miR-126	8.1E-03	0.65	27/101	4.04E-03	ANP32B (april), HSPA4, RLI, LIV-1 (SLC39A6), PTP-MEG2, CD97, DHPR	Regulation of cellular protein metabolic process
					NFKBIA, NMI, MDH1, PDCD2	Response to stress
					SMAD6, ATP6AP2, ANP32B (april), NMI, HSPA4	Apoptosis
hsa-miR-325	8.7E-03	0.20	18/63	2.03E-04	TRADD, CREST, NEDD8, annexin IV, GPX2, PDF, TNFAIP1	Developmental process
					Glypican-3, ID1, PC-TP,	Multicellular organismal development
					SNRPB (Sm-B)	RNA splicing

*Ratio of HCC-B, HCC-C, CH-B, and CH-C to normal.
†The number of significant genes ($P < 0.05$) out of predicted target genes in which expression was evaluated in microarray.
‡Statistical assessment of presence of differentially expressed genes out of predicted target genes of miRNAs.
§Representative differentially expressed genes out of predicted target genes of miRNAs.
¶Representative pathway of differentially expressed genes out of predicted target genes of miRNAs.

the hypergeometrical distribution based on gene ontology terms. Because one gene is frequently involved in multiple pathways, all pathways corresponding to the genes with significance probability were listed.

Verification of Regulation of Candidate Target Genes by miRNAs. Anti-miRNA (Ambion) specific to 13 miRNAs (has-miR-17*, has-miR-20a, has-miR-23a, has-miR-26a, has-miR-27a, has-miR-29c, has-miR-30a, has-miR-92, has-miR-126, has-miR-139, has-miR-187, has-miR-200a, and has-miR-223) showing significant differences in expression were transfected into Huh7 cells using TransMessenger transfection reagent (QIAGEN, Valencia, CA), and loss of function of each miRNA was evaluated. Similarly, precursor miRNAs of five miRNAs (has-miR-23a, has-miR-26a, has-miR-27a, has-miR-92, and has-miR-200a) were also transfected into Huh7 cells, and gain of function of each miRNA was evaluated. The loss- and gain-of-function of miRNAs were evaluated via RTD-PCR. In addition, different gene expressions regulated by miRNAs were also evaluated via RTD-PCR.

HBV/HCV Infection Model Using Cultured Cells. The plasmid pHBV 1.2 coding the 1.2-fold length of the HBV genome was transfected into Huh7.5 cells using Fugene6 transfection reagent (Roche Applied Science, Indianapolis, IN). HBeAg production in culture medium was measured using Immunis HBeAg/Ab EIA (Institute of Immunology Co., Ltd., Tokyo, Japan).[13] The amount of HBV-DNA was measured via RTD-PCR (Supplementary Fig. 1A,B). JFH1-RNA was transfected into Huh7.5 cells using TransMessenger transfection reagent (QIAGEN) and the expression of the core protein was examined via immunofluorescence staining using anti-HCV core antibody (Affinity BioReagent, CO).[14,15] HCV-RNA amount was also measured via RTD-PCR (Supplementary Fig. 1A,B). JFH1/GND was used as a negative control. miRNA expression was quantitated by RTD-PCR 48 hours after transfection.

Results

Expression of miRNA in Liver Tissue. A panel of miRNA was successfully amplified from liver tissues via RTD-PCR. The representative amplification profile of miRNA as determined with RTD-PCR is shown in Fig. 1. To assess the reliability and reproducibility of this assay system, we first measured RNU6B in duplicate from all samples in different plates. The mean difference in Ct values of RNU6B expression within the same samples was 0.08 ± 0.05 (mean $\pm$ standard deviation), indicating the high reproducibility of this assay. All Ct values from each reaction were collected, and Ct variation obtained by each probe from all patients was calculated. Although RNU6B was frequently used as the internal control, the standard Ct variation was relatively high (Ct, 27 ± 1.94), suggesting that the variances in its value depend on the state of liver disease (N, CH and HCC). Therefore, we selected has-miR-328 as the internal control with the smallest standard deviation (Ct, 30 ± 0.60). The relative expression ratio of individual miRNA to has-miR-328 was calculated and applied to the following analysis using a BRB-array tool.

Hierarchical cluster analysis revealed that the expression profiles of the 188 miRNAs from each patient were roughly classified into normal liver, HBV-infected liver (CH-B+HCC-B; HBV group), and HCV-infected liver (CH-C+HCC-C; HCV group) (Fig. 2A). HCV viremia in two patients with CH-C was persistently cleared by interferon therapy before HCC development. The background liver of one of these patients was clustered in the normal group and those of others in the HCV group. Although these two patients were not clearly differentiated from others, some miRNAs such as miR-194, miR-211, and miR-340 that were down-regulated in the HCV group were significantly up-regulated in two patients (Fig. 3, cluster 2).

The present CH and HCC expression data were obtained from the same patient; however, each sample clustered irrespective of pairs in all but two patients. miRNA expression profiling was therefore more dependent on the disease condition than on the paired condition, as also confirmed by the Dunnett test.[12] We then attempted to classify the expression profiles into HBV and HCV groups using supervised learning methods (Table 2-1). HBV and HCV groups were significantly differentiated at an 87% accuracy ($P < 0.001$). The normal liver and CH (CH-B + CH-C) and CH and HCC (HCC-B + HCC-C) were also significantly differentiated at a 90% rate of accuracy. These results suggest that different stages of liver disease (normal, CH, and HCC) can be differentiated from each other based on the miRNA expression profile, as well as HBV and HCV infection.

To examine the relationship among five categories of groups, namely, N, CH-B, CH-C, HCC-B and HCC-C, we attempted to differentiate the five groups using a supervised learning algorithm (binary tree classification) used for classifying three or more groups. SVM was used as a prediction method. Expression profiles were first classified into groups N (normal) and non-N (non-normal) (CH-C, CH-B, HCC-C, and HCC-B) (node 1) ($P < 0.01$). The non-N group was then classified into HBV and HCV (node 2) ($P < 0.01$). The HBV group was further classified into CH-B and HCC-B (node 3) ($P < 0.01$), and the HCV group was further classified into CH-C and HCC-C (node 4) ($P < 0.01$) (Fig. 2B, Table 2-2). Thus, the findings support the notion that differences in miRNA expression between HBV and HCV are as distinct as those between CH and HCC.

Out of 20 miRNAs that differentiated node 1 classification (Table 2-2), 12 also differentiated node 3 or node 4 classification. The remaining eight miRNAs specifically differentiated node 1 classification. They were down-regulated in the HBV and HCV groups compared with the normal group (Fig. 3, cluster 1). Nineteen miRNAs differentiated node 2 classification (Table 2-2) and the hierarchical clustering using these miRNAs clearly differentiated the HBV and HCV groups (Fig. 3, cluster 2). There were 15 and 14 miRNAs that differentiated node 3 and 4 classifications, respectively (Table 2-2). Hierarchical clustering using these miRNAs revealed that these miRNAs differentiated CH-B and HCC-B as well as CH-C and HCC-C, respectively; 17 miRNAs were down-regulated in HCC, and six were up-regulated in HCC (Fig. 3, cluster 3).

Table 3-2. Differentially Expessed miRNA Between HCC-B, CH-B, and HCC-C, CH-C, and Their Representative Target Genes (Cluster 2)

miRNA	Parametric *P* Value	Ratio*	No. of Significant Genes/Predicted Target Genes†	Hotelling Test *P* Value‡	Differentially Expressed Target Genes§	Pathway of Regulated Genes¶
hsa-miR-190	1.2E-05	2.06	21/68	4.47E-02	Chk1, C2orf25, VRK2, USP16, STAF65(gamma)	Regulation of cell cycle
					AP1S2, RNASE4	Mitotic cell cycle
					PPP2R1B, ARHGAP15, UBPY	Negative regulation of apoptosis
hsa-miR-134	2.3E-04	5.74	11/58	3.40E-06	VKDGC, SH2B, MALS-1, DDB2	Multicellular organismal process
					BCRP1	Regulation of viral reproduction
					DDB2	Lipid biosynthetic process
hsa-miR-151	2.8E-04	1.82	12/62	6.41E-01	RGS2, UFO, AK2, USP7	G-protein signaling
					eIF4G2, USP7	Regulation of translation
					SLC22A7	Organic anion transport
hsa-miR-193	5.0E-04	1.67	23/95	9.30E-01	G-protein alpha-11, p130CAS, VAV-1, PDCD11	Cell motility
					Colipase, ACSA	Energy coupled proton transport
					DCOR	Intracellular signaling cascade
hsa-miR-133b	1.7E-03	2.42	20/97	3.69E-02	DDB2, Bcl-3, Cystatin B	Proteasomal protein catabolic process
					Rab-3, RAG1AP1, KCNH2, DCOR	Regulation of biological quality
					AL1B1	Carbohydrate metabolic process
hsa-miR-324-5p	2.9E-03	1.51	27/121	1.90E-06	SKAP55, VAV-1, DDB2, E2A, NIP1	Cellular developmental process
					MEMO (CGI-27), Rab-3	Cellular structure morphogenesis
					COPG1, GPX3, OAZ2	Glutathione metabolic process
hsa-miR-182*	3.1E-03	2.23	28/123	< 1e-07	Alpha-endosulfine, HCCR-2, Thioredoxin-like 2, TPT1, USP7	Translation initiation in response to stress
					DDB2, TPT1	Cellular developmental process
					JIP-1	JNK cascade
hsa-miR-105	4.6E-03	4.38	18/68	4.74E-05	Beta-2-microglobulin, HLA-B27	Antigen processing and presentation
					PIMT, IL-17RC	Immune response
					MHC class I, CDK9, ERG1, Desmocollin 3	
hsa-miR-211	5.3E-03	25.61	10/56	2.00E-04	PSMD5, SLC26A6	Proteasomal protein catabolic process
hsa-miR-20	5.7E-03	1.52	27/113	5.28E-03	Noelin, SC4MOL, Thioredoxin-like 2, CCL5, NALP3	Regulation of apoptosis
					Hic-5/ARA55, USP16, MAP4, Ferroportin 1	Positive regulation of cellular process
					TOP3A, PLRP1	Oxygen transport
hsa-miR-191	6.7E-03	1.39	25/79	7.55E-04	CDK9, GPS2, CLTA, LXR-alpha	Nucleic acid metabolic process
					ACSA	Acetyl-CoA biosynthetic process
					UGCGL1, SGPP1	Metal ion transport
hsa-miR-340	8.5E-03	1.48	17/81	3.73E-03	FKBP12, DCOR,	Calcium ion transport
					Gelsolin, VAV-1, ARF6	Actin cytoskeleton organization and biogenesis
					HXK3	Glucose catabolic process
hsa-miR-194	8.7E-03	1.67	13/74	5.90E-01	Cyclin B1, Serglycin	M phase of mitotic cell cycle
					PTE2	Acyl-CoA metabolic process
					SLC7A6	Carbohydrate utilization
hsa-miR-23a	1.9E-04	0.46	14/97	< 1e-07	*RGL2*, MANR, MEK1 (MAP2K1), Caspase-3, AZGP1	Protein kinase cascade
					FRK, Pyk2(FAK2), CSE1L	Cellular developmental process
					AZGP1	Defense response
hsa-miR-142-5p	4.9E-04	0.40	25/89	9.10E-06	Sirtuin4, PAI2, PSAT, RIL, CDC34, SPRY1	Metabotropic glutamate receptor
					E4BP4, DNAJC12, WWP1, PAIP1, PASK, rBAT	Regulation of gene expression
					VCAM1, CaMK I, WWP1, FHL3	Cell-matrix adhesion
hsa-miR-34c	5.1E-04	0.20	31/129	7.30E-06	Diacylglycerol kinase, zeta, PLC-delta 1, ATP2C1, PAI2	Manganese ion transport
					MLK3(MAP3K11), MEK1(MAP2K1), CDC25C, MRF-1, XPC	Protein kinase cascade
					GNT-IV	Inflammatory cell apoptosis

Table 3-2. Continued

miRNA	Parametric *P* Value	Ratio*	No. of Significant Genes/Predicted Target Genes†	Hotelling Test *P* Value‡	Differentially Expressed Target Genes§	Pathway of Regulated Genes¶
hsa-miR-124b	8.6E-04	0.32	25/120	7.10E-05	E2F5, Rad51, Jagged1	Muscle development
					MLK3(MAP3K11), RGS1	Intracellular signaling cascade
					COL16A1	MAPKKK cascade
hsa-let-7a	1.0E-03	0.45	28/136	9.35E-04	RAD51C, CoAA, hASH1, Cockayne syndrome B, Caspase-1, PP5	Response to DNA damage stimulus
					PLC-delta 1, MANR, ACADVL	Fibroblast proliferation
					HGF, NGF	Cellular developmental process
hsa-miR-27a	3.9E-03	0.59	18/108	1.19E-02	COL16A1, RIL, RhoGDI gamma, ANP32B (april)	Cytoskeleton organization and biogenesis
					VE-cadherin, NTH1, GATA-2, E4BP4	Response to external stimulus
					RAD51C	DNA recombination

*Ratio of HCC-B, CH-B, to HCC-C,CH-C.
†The number of significant genes ($p < 0.05$) out of predicted target genes in which expression was evaluated in microarray.
‡Statistical assesment of presence of differentially expressed genes out of predicted target genes of miRNAs.
§Representative differentially expressed genes out of predicted target genes of miRNAs.
¶Representative pathway of differentially expressed genes out of predicted target genes of miRNAs.

These results indicate that there were two types of miRNAs—one associated with HBV and HCV infection (cluster 2), the other associated with the stages of liver disease (clusters 1 and 2) that were irrelevant to the differences in HBV and HCV infection.

Differential miRNAs and Their Candidate Target Genes and Signaling Pathways. Differentially expressed miRNAs are shown in Table 3. In addition to the expression ratios of miRNAs in each group, the number of genes analyzed on the microarray predicted to be the target genes of miRNAs and that which actually showed significant ($P < 0.05$) differences in expression are also shown. Based on the frequencies and levels of expression of differential genes, the significance of regulation of these gene groups by miRNAs was evaluated using Hotelling T2 test (BRB ArrayTools) (Table 3). The representative candidate target genes and their signaling pathways by each miRNA were shown one by one (Table 3). The signaling pathways regulated by all differential miRNAs in each category of groups are shown in Table 4.

Eight miRNAs were down-regulated in the HBV and HCV groups compared with the normal group (Table 3-1; Fig. 3, cluster 1). These miRNAs were associated with an increased expression of genes related to cell adhesion, cell cycle, protein folding, and apoptosis (Tables 3-1, 4-1), and possibly with the common feature of CH irrespective of the differences in HBV and HCV infection.

Nineteen miRNAs clearly differentiated the HBV and HCV groups (Fig. 3, cluster 2, Table 3-2). Thirteen miRNAs exhibited a decreased expression in the HCV group, and six showed a decreased expression in the HBV group. miRNAs exhibiting a decreased expression in the HCV group regulate genes related to immune response, antigen presentation, cell cycle, proteasome, and lipid metabolism. On the other hand, those exhibiting a decreased expression in the HBV group regulate genes related to cell death, DNA damage and recombination, and transcription signals. These findings reflected the differences in the gene expression profile between CH-B and CH-C described (Tables 3-2, 4-2).[10] Interestingly, although these miRNAs were HBV and HCV infection–specific, some of them were reported to be tumor-associated miRNAs, suggesting the possible involvement of infection-associated miRNAs in HCC development.

Twenty-three miRNAs clearly differentiated CH and HCC that were irrelevant to the differences in HBV and HCV infection. Seventeen miRNAs were down-regulated in HCC that up-regulated cancer-associated pathways such as cell cycle, adhesion, proteolysis, transcription, translation, and the Wnt signaling pathway (Tables 3-3, 4-3). Six miRNAs were up-regulated in HCC that down-regulated all inflammation-mediated signaling pathways, potentially reflecting impaired antitumor immune response.

Relationship Between Expressions of Infection-Associated miRNA in Liver and Cultured Cells Infected with HBV and HCV. To clarify whether the expression of infection-associated miRNA is regulated by HBV and HCV infection, we investigated the relationship between changes in miRNA in liver tissues and those in miRNA in Huh7.5 cells in which infectious HBV or HCV clones replicated. To evaluate the replication of each clones in Huh7.5 cells, we measured time-course changes in the amounts of HBV-DNA and HCV-RNA in Huh7.5 cells transfected with pHBV1.2 and JFH1-RNA, respectively, by RTD-PCR (Supplementary Fig. 1A). The expression of HBV proteins was examined by measuring the amount

Table 3-3. Differentially Expessed miRNA Between CH and HCC and Their Representative Target Genes (Cluster 3)

miRNA	Parametric p-value	Ratio*	No. of Significant Genes/Predicted Target Genes†	Hotelling Test *P* Value‡	Differentially Expressed Target Genes§	Pathway of Regulated Genes¶
hsa-miR-139	4.50E-06	0.42	19/106	2.70E-03	Cyclin B1, DHX15, MCM5, Histone H2A	Mitotic cell cycle
					RBCK1, SYHH	Protein catabolic process
					ILK, IGFBP7, SAFB, CTR9	Response to external stimulus
hsa-miR-30a-3p	2.50E-05	0.49	26/144	1.73E-02	GGH, Pirin, ZNF207, Annexin VII	Regulation of oxidoreductase activity
					ILK, LTA4H, ABC50, GNPAT	Cell-matrix adhesion
					DLC1	Morphogenesis
hsa-miR-130a	7.00E-05	0.50	22/108	1.07E-02	SPHM, PPP2R5D, RHEB2, SPHM	Mitotic cell cycle
					MLK3(MAP3K11), Otubain1, TIMP4	Protein modification process
					NRBP	Cell differentiation
hsa-miR-223	3.40E-04	0.39	14/90	6.52E-03	Ephrin-A1, Midkine, FDPS	Cell morphogenesis
					K(+) channel, subfamily J	Notch signaling pathway
hsa-miR-187	3.55E-04	0.12	16/66	6.76E-04	HFE2, Otubain1	Negative regulation of programmed cell death
					PRSS11, SUPT5H, RAG1AP1	Developmental process
					PLOD3	Mitochondrial ornithine transport
hsa-miR-200a	6.86E-04	0.18	20/141	2.15E-02	*CDC25B, KAP3, CDK2AP2,* CHKA	Cell communication
					POLD	DNA replication
					CPSF4	RNA splicing
hsa-miR-17-3p	8.42E-04	0.58	28/108	8.98E-04	MLK3(MAP3K11), Tip60, ACBD6, DOC-1R, DAX1, RBCK1	Protein kinase cascade
					WNT5A, 14-3-3 gamma, DHX15	BMP signaling pathway
					HFE2, MCM5	DNA recombination
hsa-miR-99a	1.17E-03	0.53	33/163	9.52E-03	Calpain small subunit, Thoredoxin-like 2, Survivin	Cytokinesis
					IBP2, DNA-PK, KAP3,	Intracellular signaling cascade
					NFE2L1, PARP-1, HDAC11	Regulatory T cell differentiation
hsa-miR-200b	1.57E-03	0.18	24/147	2.72E-02	HSP47, HMG2, NRBP	Regulation of cell cycle
					SNX17	Cell motility
					Ephrin-A1	Receptor protein signaling pathway
hsa-miR-125b	1.82E-03	0.55	26/114	1.03E-01	COL4A2, TIP30, HSP47, MSP58	Cell adhesion
					MLK3(MAP3K11), ERK2 (MAPK1), ERK1 (MAPK3), PLOD3	Nuclear translocation of MAPK
					Otubain1, SCN4A(SkM1)	Ubiquitin-dependent protein catabolic process
hsa-miR-30e	2.10E-03	0.65	24/151	4.30E-02	Cyclin B1, XTP3B, GAK, Annexin VII, MIC2, NRBP	Mitotic cell cycle
					MSS4	Protein localization
					S100A10	Calcium ion transport
hsa-miR-199a*	4.26E-03	0.35	11/71	7.16E-02	BUB3, Cyclin B1, LMNBR	Mitotic cell cycle
					PRAME	Cardiac muscle cell differentiation
hsa-miR-122a	6.31E-03	0.51	11/80	1.01E-03	JAB1, APEX, Clathrin heavy chain	Base-excision repair
					PARN	Translational initiation
					DDAH2	Regulation of cellular respiration
hsa-miR-199a	8.77E-03	0.35	18/94	3.56E-02	IL-13, MLK3(MAP3K11), CLK2, ACP33	Protein amino acid phosphorylation
					PAFAH beta, SPA1, CLCN4	Small GTPase mediated signal transduction
hsa-miR-326	9.00E-03	0.57	29/147	2.25E-01	Midkine, ENT1, IP3KA, PSMC5, ANCO-1	Regulation of programmed cell death
					Thy-1, MCM6, Tip60, VILIP3	Cell-matrix adhesion
					COMP, Cathepsin A	Blood vessel development
hsa-miR-92	9.60E-03	0.81	28/140	2.47E-02	*TUBGCP2,* Fibrillin 1, PIPKI gamma, KAP3	Rho protein signal transduction
					SNX15, BCAT2	LDL receptor and BCAA metabolism
					IGFBP7, FZD6, COPS6	Adenosine receptor signaling pathway
hsa-miR-221	3.40E-06	3.34	16/67	3.59E-01	Lck, Kallistatin, Neuromodulin, LFA-3, PA24A, AZGP1, MSH2	Immune response-activating signal transduction
					KYNU, PMCA3	DNA repair

Table 3-3. *Continued*

miRNA	Parametric p-value	Ratio*	No. of Significant Genes/Predicted Target Genes†	Hotelling Test *P* Value‡	Differentially Expressed Target Genes§	Pathway of Regulated Genes¶
hsa-miR-222	6.50E-06	2.23	18/85	1.59E-02	Thrombospondin 1, Lck, MSH2, ATF-2, CITED2, Kallistatin	Cell motility
					PGAR	Triacylglycerol metabolic process
					KYNU	DNA replication
hsa-miR-301	5.22E-05	1.96	14/71	1.16E-01	Beta-2-microglobulin, PPCKM, PRC, Fra-1, PPCKM, ACAT2	Antigen processing and presentation
					BMPR1B, ARMER, EHM2, RBBP8	Meiotic recombination
					Neuromodulin, LDLR	Cell motility
hsa-miR-21	7.67E-03	1.57	19/81	1.86E-04	Btk, Fra-1, MSH2, Collectrin, Adipophilin	Regulation of T cell proliferation
					RNASE4, AGXT2L1	Peptidyl-tyrosine phosphorylation
					SARDH	Natural killer cell activation during immune response
hsa-miR-183	2.46E-02	3.51	13/86	3.36E-01	Hdj-2, PEMT, Lck, MKP-5, Chondromodulin-I, ABCA8	Cell differentiation
					IL-16, MTRR, SerRS	Methionine biosynthetic process
hsa-miR-98	5.22E-02	1.32	24/130	2.95E-04	ACAA2, LTB4DH, ACADVL, DECR, S14 protein,	Fatty acid metabolic process
					Rapsyn, Kallistatin, ENPEP, Beta crystallin B1	Multicellular organismal process
					CYP4F8	Prostaglandin metabolic process

*Ratio of HCC to CH.
†The number of significant genes ($P<0.05$) out of predicted target genes in which expression was evaluated in microarray.
‡Statistical assesment of presence of differentially expressed genes out of predicted target genes of miRNAs.
§Representative differentially expressed genes out of predicted target genes of miRNAs.
¶Representative pathway of differentially expressed genes out of predicted target genes of miRNAs.

of HBeAg released in culture medium (Supplementary Fig. 1B). HCV protein expression was examined by evaluating the core protein expression after 48 hours by fluorescence immunostaining (Supplementary Fig. 1C). RNA was extracted from the Huh7.5 cells 48 hours after gene transfection, and miRNA expression pattern in the cells was compared with those in liver tissues. We found a strong correlation between differences in miRNA expression between liver tissues of the HBV and HCV groups, and those in miRNA expression between Huh7.5 cells transfected with HBV and HCV clones ($r = 0.73$, $P = 0.0006$) (Fig. 5). These results revealed that differences in the expression of infection-associated miRNA in the liver between the HBV and HCV groups are explained by changes in miRNA expression caused by HBV and HCV infections.

Verification of Regulation of Candidate Target Genes by miRNA. Anti-miRNAs (Ambion) specific to 13 miRNAs (has-miR-17*, has-miR-20a, has-miR-23a, has-miR-26a, has-miR-27a, has-miR-29c, has-miR-30a, has-miR-92, has-miR-126, has-miR-139, has-miR-187, has-miR-200a, and has-miR-223) showing significant differences in expression were transfected into Huh7 cells to examine loss of function of the miRNAs. Five miRNAs (has-miR-23a, has-miR-26a, has-miR-27a, has-miR-92, and has-miR-200a) showed a decreased expression by more than 50%. Precursor miRNAs of these miRNAs were also transfected into the cells to examine the gain of function of the miRNAs (Supplementary Fig. 2). It was confirmed that the expressions of target genes of the five miRNAs (LIG4 [by has-miR-26a]; RGL2 [by has-miR-23a]; Rad51C [by has-miR-27a]; KAP3, CDC25B, KAP3, CDK2AP2, POLD, and CPSF4 [by has-miR-200a]; and TUBGCP2, SNX15 and BCAT2 [by has-miR-92]) were increased by the suppression of the miRNAs induced by anti-miRNAs and were decreased by the overexpression of precursor miRNAs (Supplementary Fig. 3).

Discussion

miRNA plays an important role in various diseases such as infection and cancer.[1-3] In this study, we examined miRNA expression profiles in normal liver and HCC, including nontumor lesions infected with HBV or HCV. Although the expression profiles of miRNAs in HCC have been reported,[16-18] most of the studies were performed using a microarray system. Because we thought that miRNAs could not produce enough detection signals owing to their short length, we applied a highly sensitive and quantitative RTD-PCR method for miRNAs. Moreover, global gene expression in the same tissues was ana-